Supplementary Materials

AACVD Synthesized Tungsten Oxide-NWs loaded with Osmium oxide as Gas Sensor Array: Enhancing Detection with PCA and ANNs

Alejandro Santos-Betancourt [1,2,3], Èric Navarrete [1], Damien Cossement [4], Carla Bittencourt [5], and Eduard Llobet [1,2,3*]

[1] Universitat Rovira i Virgili, Microsystems Nanotechnologies for Chemical Analysis (MINOS), Departament d'Enginyeria Electrònica, Països Catalans, 26, 43007 Tarragona, Catalunya, Spain

[2] IU-RESCAT, Research Institute in Sustainability, Climatic Change and Energy Transition, Universitat Rovira i Virgili, Joanot Martorell 15, 43480 Vila-seca, Spain

[3] TecnATox - Centre for Environmental, Food and Toxicological Technology, Universitat Rovira i Virgili, Avda. Països Catalans 26, 43007 Tarragona, Spain

[4] Materia Nova Research Center, Parc Initialis, Avenue Copernic 3, 7000 Mons, Belgium

[5] Chimie des Interactions Plasma – Surface (ChIPS), Research Institute for Materials Science and Engineering, Université de Mons, Parc Initialis, Avenue Copernic 3, 7000 Mons, Belgium

[*] Corresponding author

Figure S1 shows (upper panel) an EDX analysis conducted on a sensor sample. The osmium loaded tungsten oxide film coats an alumina substrate. Peaks corresponding to the tungsten oxide film and the alumina substrate clearly appear. However, osmium is not detected. (lower panel) quantitative results of the microanalysis.

The experiment conditions were:

Live Time: 40.0 sec

Filter Fit   Chi Squared:13.977   Errors: +/- 1 Sigma

Correction Method: Proza (Phi-Rho-Z) Acc.Voltage: 20.0 kV

Take Off Angle: 34.9 deg.

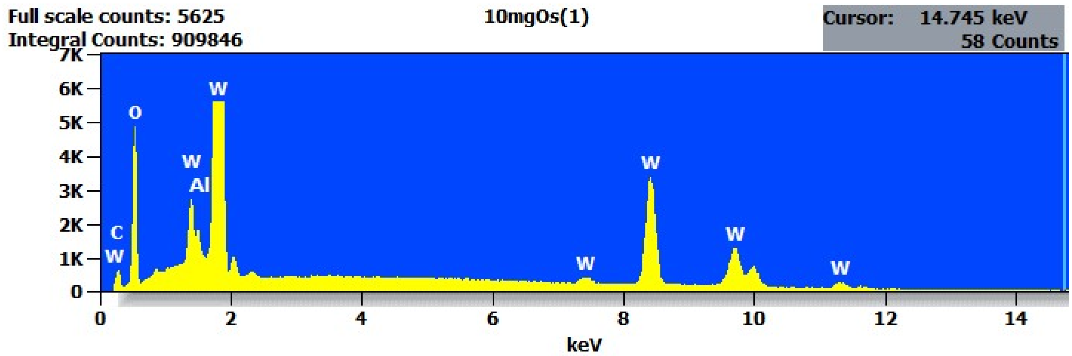

Element	Weight %	Weight % Error	Norm. Wt.%	Atom %	Formula
C	2.53	± 0.04	2.53	11.32	C
O	19.17	± 0.15	19.17	64.37	O
Al	0.84	± 0.04	0.84	1.68	Al
W	77.45	± 0.79	77.45	22.63	W
Total	100.00		100.00	100.00	

Figure S1: EDX performed to a sensor sample consisting of WO_3 decorated with osmium.

Figure S2 shows the results of a different EDX analysis conducted on an osmium loaded tungsten oxide sample deposited on a TEM grid (lacey carbon film supported on nickel). Similarly to the previous EDX analysis performed on a sensor sample, this analysis is inconclusive for the presence of osmium in osmium-loaded samples.

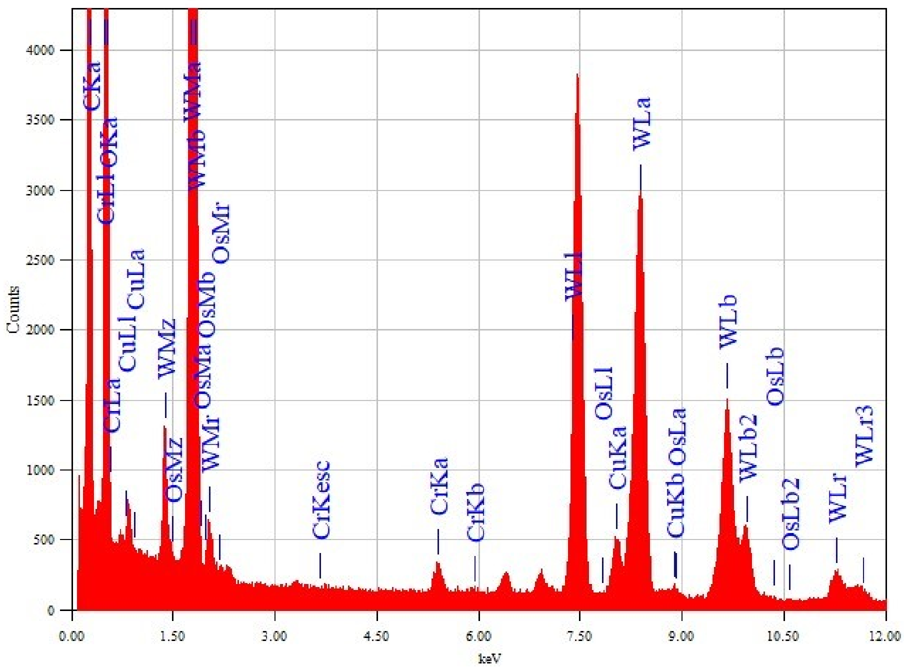

Figure S2: EDX analysis performed to an WO_3 decorated with osmium deposited on a TEM grid.

On the use of ToF-SIMS to confirm the presence of osmium oxide in the samples

An XPS analysis of the different samples was performed. However, the amount of Os that loaded the tungsten oxide was found to be under the sensitivity of the XPS technique and this for the two types of samples produced. The calculated detection limit of Osmium by XPS is 1.5 ppm. Therefore, to evaluate the presence of Osmium, the ToF-SIMS technique was employed, which is more sensitive technique than XPS, as it enables detecting the presence of chemical species at trace levels, down to ppb concentrations. However, unlike XPS, the ToF-SIMS is a qualitative technique, which has enabled confirming the presence of Os in the loaded tungsten oxide samples, but that does not allow for a proper quantitative analysis of this loading. Additionally, the TOF-SIMS analyses were performed in *spectrometry mode* (not in *imaging mode*), with a lateral resolution of roughly 1-2 µm. Therefore, it is not possible to determine the characteristic size and morphology of the Osmium clusters.

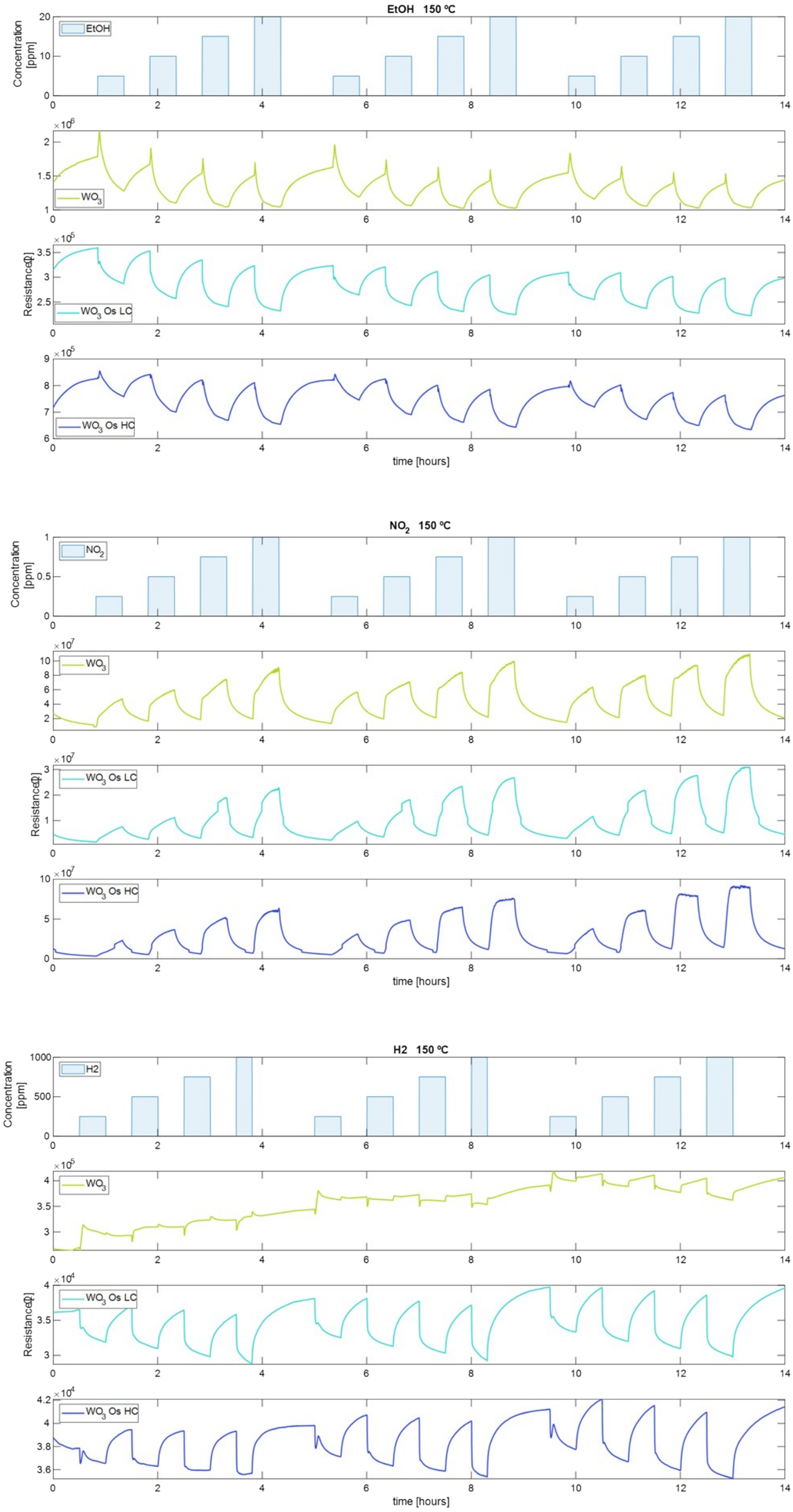

Figure S3: Measurements at 150˚ C of (up) EtOH, (middle) NO_2, and (down) H_2.

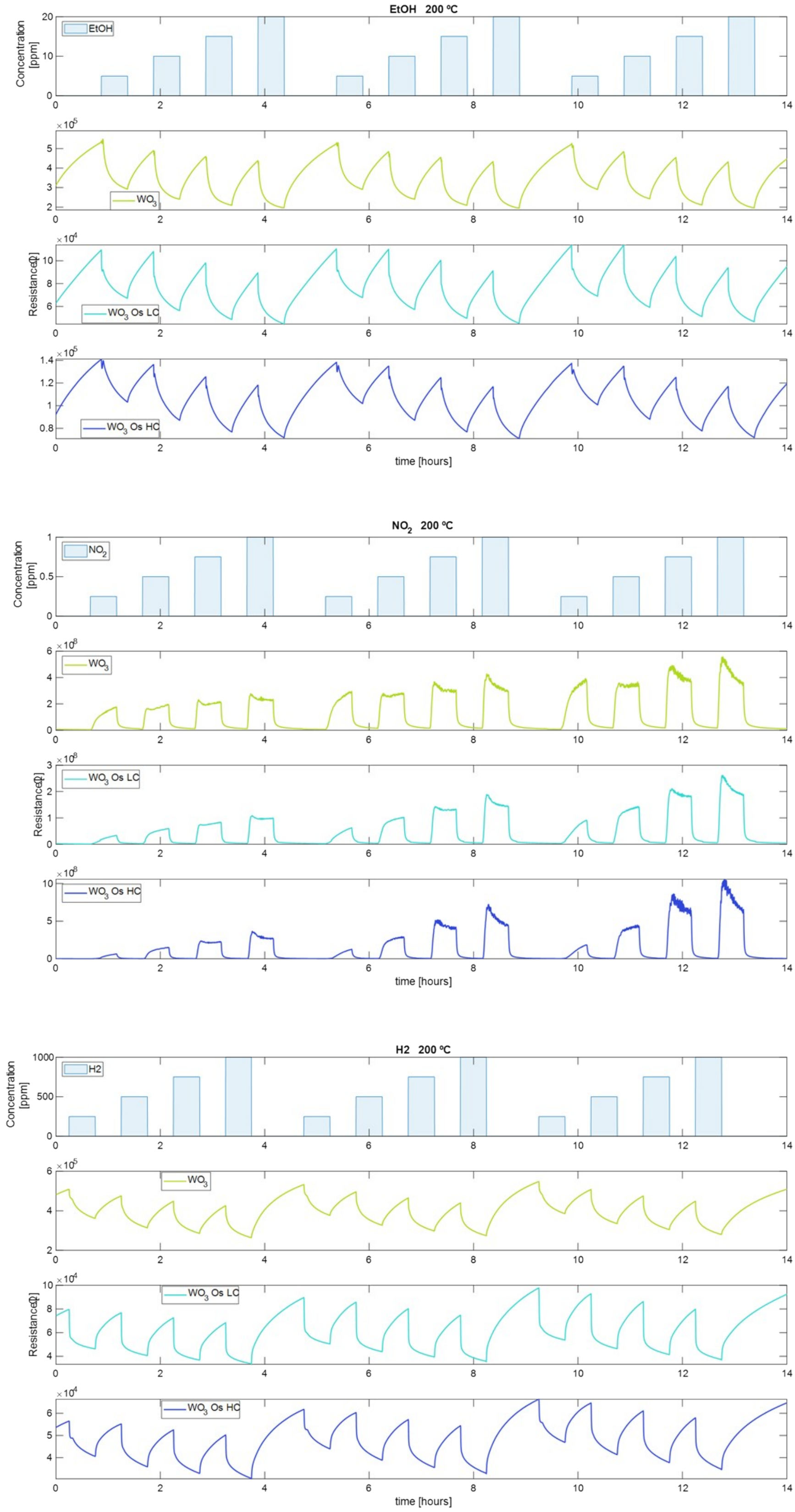

Figure S4: Measurements at 200˚ C of (up) EtOH, (middle) NO_2, and (down) H_2.

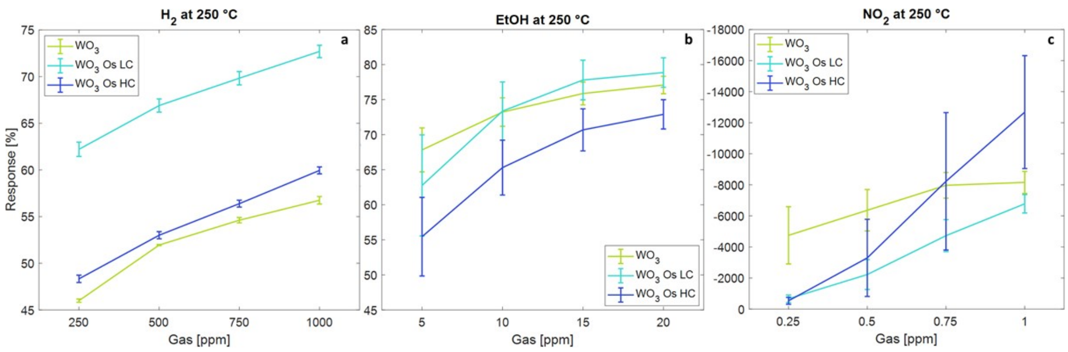

Figure S5: Calibration curves at 250˚ C of (a) H_2, (b) EtOH, and (down) NO_2.

Table S1: Summary of the statistics of sensor measurements.

Sensor	Gas	Temperature [˚C]	Concentration [ppm]	Response Mean [%]	Response Error [%]	Abs. Error [ppm]	Rel. Error [%]
pure	NO_2	250	0.25	-4749.6	1843.1	-0.24	-95.03
pure	NO_2	250	0.5	-6364.0	1336.0	-0.26	-52.24
pure	NO_2	250	0.75	-7970.8	825.4	-0.21	-27.45
pure	NO_2	250	1	-8160.0	710.0	-0.21	-21.05
pure	H_2	250	250	46.0	0.18	6.35	2.54
pure	H_2	250	500	52.0	0.06	3.65	0.73
pure	H_2	250	750	54.6	0.29	26.45	3.53
pure	H_2	250	1000	56.8	0.40	47.00	4.70
pure	EtOH	250	5	67.8	3.1	2.47	49.35
pure	EtOH	250	10	73.2	2.0	2.99	29.88
pure	EtOH	250	15	75.9	1.6	3.45	23.00
pure	EtOH	250	20	77.1	1.2	3.43	17.13
WO_3OsLC	NO_2	250	0.25	-667.4	239.8	-0.05	-19.16
WO_3OsLC	NO_2	250	0.5	-2227.7	964.5	-0.13	-26.37
WO_3OsLC	NO_2	250	0.75	-4728.7	1030.8	-0.11	-15.05
WO_3OsLC	NO_2	250	1	-6779.3	592.4	-0.06	-5.54
WO_3OsLC	H_2	250	250	62.2	0.76	27.71	11.09
WO_3OsLC	H_2	250	500	66.9	0.71	47.60	9.52
WO_3OsLC	H_2	250	750	69.8	0.71	68.86	9.18
WO_3OsLC	H_2	250	1000	72.7	0.66	82.51	8.25
WO_3OsLC	EtOH	250	5	62.8	7.2	3.41	68.12
WO_3OsLC	EtOH	250	10	73.4	4.2	3.50	35.04
WO_3OsLC	EtOH	250	15	77.8	2.8	3.34	22.29
WO_3OsLC	EtOH	250	20	78.9	2.1	3.16	15.81
WO_3OsHC	NO_2	250	0.25	-536.8	222.5	-0.03	-12.07
WO_3OsHC	NO_2	250	0.5	-3298.1	2481.5	-0.19	-37.38
WO_3OsHC	NO_2	250	0.75	-8228.1	4423.3	-0.24	-31.50
WO_3OsHC	NO_2	250	1	-12681.6	3635.6	-0.15	-15.21
WO_3OsHC	H_2	250	250	48.3	0.40	13.40	5.36
WO_3OsHC	H_2	250	500	53.0	0.38	23.26	4.65
WO_3OsHC	H_2	250	750	56.4	0.37	31.58	4.21

WO_3OsHC	H_2	250	1000	60.0	0.37	40.86	4.09
WO_3OsHC	EtOH	250	5	55.5	5.6	2.52	50.37
WO_3OsHC	EtOH	250	10	65.3	3.9	3.07	30.68
WO_3OsHC	EtOH	250	15	70.7	3.0	3.25	21.68
WO_3OsHC	EtOH	250	20	72.9	2.1	2.85	14.27

Table S2: Summary of the performance of the classification algorithms.

Number hidden layers	Number of neurons per layer	Activation function	Accuracy training [%]	Accuracy test [%]	Working Temperature (˚ C)
3	**10**	**Tanh**	**93.58**	**93.82**	**150**
3	10	Sigmoid	92.91	92.09	150
3	10	ReLU	91.02	86.56	150
1	10	ReLU	90.16	86.70	150
1	100	ReLU	90.06	86.78	150
1	25	ReLU	89.66	88.11	150
2	10	ReLU	89.61	91.59	150
3	10	None	81.89	81.71	150
1	**100**	**Tanh**	**91.56**	**91.60**	**200**
1	100	Sigmoid	91.28	91.47	200
3	10	ReLU	88.99	85.91	200
1	100	ReLU	88.99	88.61	200
1	25	ReLU	88.81	88.58	200
2	10	ReLU	88.63	88.26	200
1	10	ReLU	87.98	87.58	200
1	100	None	86.82	85.55	200
1	**10**	**Tanh**	**91.61**	**93.18**	**250**
1	10	ReLU	91.38	92.26	250
1	100	ReLU	91.76	92.20	250
1	25	ReLU	91.46	91.97	250
3	10	ReLU	90.23	91.45	250
1	10	Sigmoid	91.93	90.91	250
2	10	ReLU	90.29	90.82	250
1	10	None	89.69	89.45	250

Table S3: Summary of the performance of the quantification models for nitrogen dioxide.

Number hidden layers	Number of neurons per layer	Activation function	RMSE training [ppb]	R-squared training	RMSE test [ppb]	R-squared test	Working Temperature (˚ C)
3	**10**	**Tanh**	**0.09**	**0.90**	**0.07**	**0.94**	**150**
1	100	ReLU	0.10	0.88	0.09	0.90	150
3	10	ReLU	0.10	0.89	0.09	0.89	150
1	25	ReLU	0.11	0.86	0.11	0.86	150
2	10	ReLU	0.10	0.87	0.11	0.86	150
3	10	Sigmoid	0.11	0.86	0.11	0.85	150
1	10	ReLU	0.12	0.84	0.12	0.85	150
3	10	None	0.20	0.55	0.20	0.57	150
1	**100**	**ReLU**	**0.12**	**0.87**	**0.11**	**0.89**	**200**
3	10	ReLU	0.12	0.86	0.11	0.88	200
2	10	ReLU	0.12	0.86	0.12	0.87	200
1	25	ReLU	0.14	0.83	0.12	0.85	200
1	10	ReLU	0.15	0.81	0.13	0.84	200
1	100	Tanh	0.14	0.81	0.14	0.82	200
1	100	Sigmoid	0.16	0.78	0.15	0.80	200
1	100	None	0.20	0.66	0.19	0.67	200
3	**10**	**ReLU**	**0.07**	**0.94**	**0.08**	**0.94**	**250**
3	10	Tanh	0.08	0.94	0.08	0.94	250
1	100	ReLU	0.08	0.93	0.08	0.94	250
2	10	ReLU	0.08	0.93	0.08	0.94	250

1	25	ReLU	0.08	0.93	0.08	0.94	250
3	10	Sigmoid	0.09	0.92	0.08	0.93	250
1	10	ReLU	0.09	0.92	0.09	0.92	250
3	10	None	0.14	0.81	0.13	0.84	250

Table S4: Summary of the performance of the quantification models for ethanol.

Number hidden layers	Number of neurons per layer	Activation function	RMSE training [ppm]	R-squared training	RMSE test [ppm]	R-squared test	Working Temperature (˚ C)
1	**100**	**Tanh**	**1.65**	**0.94**	**1.33**	**0.96**	**150**
1	100	Sigmoid	1.67	0.94	1.58	0.94	150
1	100	ReLU	1.89	0.92	1.71	0.93	150
3	10	ReLU	1.97	0.91	1.80	0.92	150
1	25	ReLU	2.46	0.87	2.26	0.88	150
2	10	ReLU	2.03	0.91	2.28	0.88	150
1	10	ReLU	2.92	0.82	3.02	0.80	150
1	100	None	5.53	0.36	5.44	0.35	150
3	**10**	**Sigmoid**	**2.01**	**0.92**	**1.27**	**0.96**	**200**
3	10	ReLU	1.86	0.93	1.58	0.94	200
3	10	Tanh	2.03	0.91	1.71	0.94	200
1	100	ReLU	2.00	0.92	1.80	0.93	200
3	10	ReLU	2.00	0.92	1.85	0.93	200
1	25	ReLU	2.21	0.90	2.04	0.91	200
1	10	ReLU	2.42	0.88	2.11	0.91	200
3	10	None	5.24	0.46	5.04	0.49	200
3	**10**	**Tanh**	**2.32**	**0.89**	**1.64**	**0.94**	**250**
3	10	ReLU	2.48	0.88	2.04	0.91	250
1	100	ReLU	2.38	0.89	2.15	0.90	250
1	25	ReLU	2.51	0.88	2.27	0.89	250
2	10	ReLU	2.55	0.87	2.39	0.88	250
3	10	Sigmoid	2.51	0.88	2.59	0.87	250
1	10	ReLU	2.73	0.86	2.62	0.86	250
3	10	None	4.99	0.53	4.99	0.51	250

Table S5: Summary of the performance of the quantification models for hydrogen.

Number hidden layers	Number of neurons per layer	Activation function	RMSE training [ppm]	R-squared training	RMSE test [ppm]	R-squared test	Working Temperatur e (˚ C)
1	**100**	**ReLU**	**104.33**	**0.90**	**95.81**	**0.91**	**150**
2	10	ReLU	98.40	0.91	100.97	0.90	150
3	10	ReLU	97.64	0.91	105.70	0.89	150
1	25	ReLU	105.83	0.89	113.01	0.88	150
1	100	Tanh	123.15	0.86	128.10	0.84	150
1	100	Sigmoid	134.10	0.83	134.77	0.83	150
1	10	ReLU	138.01	0.82	140.21	0.81	150
1	100	None	253.72	0.41	250.01	0.42	150
1	**100**	**ReLU**	**96.48**	**0.92**	**107.92**	**0.90**	**200**
1	25	ReLU	108.21	0.90	112.29	0.89	200
2	10	ReLU	107.88	0.90	120.72	0.87	200
1	100	Sigmoid	104.76	0.90	120.72	0.87	200
3	10	ReLU	99.87	0.91	122.56	0.87	200
1	10	ReLU	115.44	0.88	130.57	0.85	200
1	100	Tanh	152.04	0.80	154.29	0.80	200
1	100	None	250.28	0.47	249.59	0.47	200
1	**100**	**ReLU**	**76.19**	**0.94**	**85.57**	**0.93**	**250**
1	100	Sigmoid	72.78	0.95	87.76	0.93	250
2	10	ReLU	74.55	0.95	91.84	0.92	250
1	25	ReLU	77.93	0.94	92.14	0.92	250
3	10	ReLU	74.79	0.95	94.41	0.92	250

1	100	Tanh	95.87	0.91	94.74	0.92	250
1	10	ReLU	79.49	0.94	95.32	0.92	250
1	100	None	255.43	0.42	259.19	0.42	250

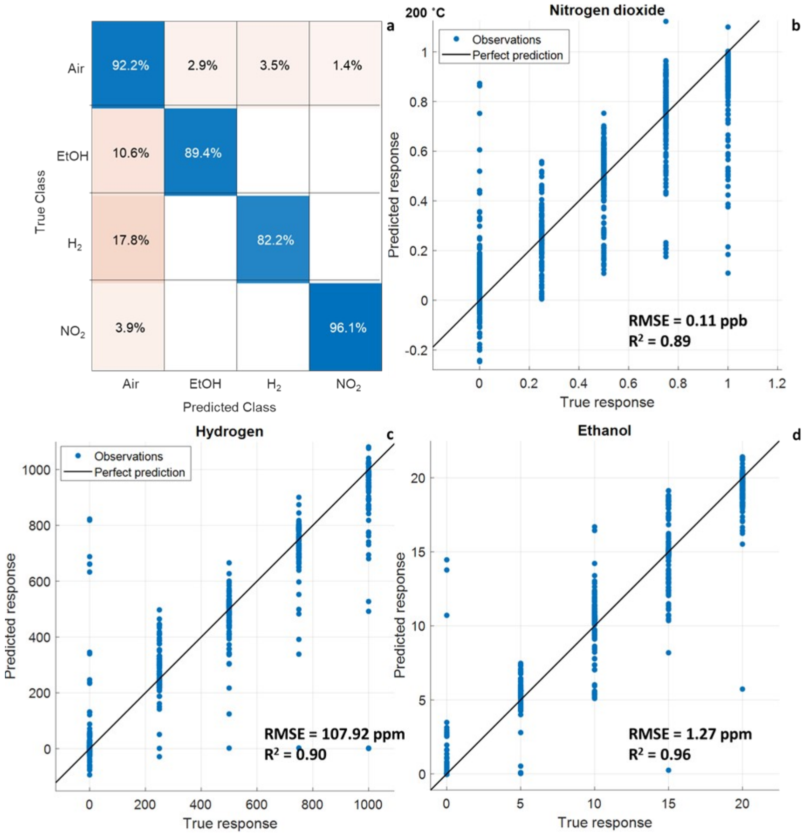

Figure S6: Results of classification and quantification models when using test dataset at 200˚ C. (a) Classification. (b) NO_2 quantification. (c) H_2 quantification. (d) EtOH quantification.

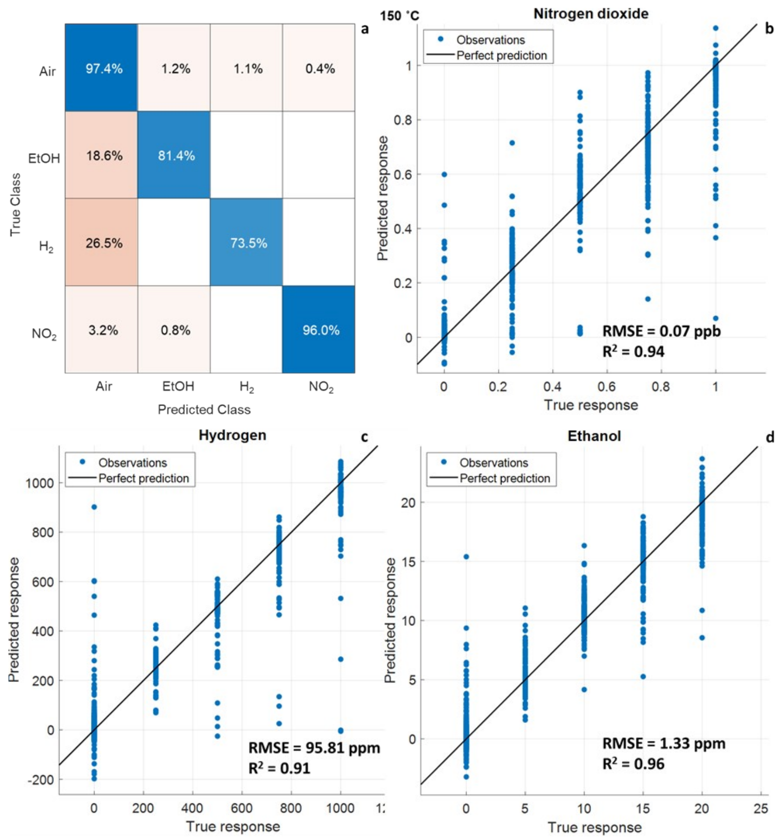

Figure S7: Results of classification and quantification models when using test dataset at 150° C. (a) Classification. (b) NO_2 quantification. (c) H_2 quantification. (d) EtOH quantification.

Table S6: Relationship between classification accuracy and working temperature of the sensors.

Working Temperature (° C)	Classifying NO_2 (%)	Classifying EtOH (%)	Classifying H_2 (%)
150	96.0	81.4	73.5
200	96.1	89.4	82.2
250	95.2	90.1	86.9

Table S7: Summary of the best quantification models for EtOH, NO_2, and H_2 at three temperatures.

Gas	Temperature [° C]	RMSE train [ppm]	R-squared train	RMSE test [ppm]	R-squared test
EtOH	150	1.65	0.94	1.33	0.96
	200	2.01	0.92	1.27	0.96
	250	2.32	0.89	1.64	0.94
NO_2	150	0.09×10^{-3}	0.90	0.07×10^{-3}	0.94
	200	0.12×10^{-3}	0.87	0.11×10^{-3}	0.89
	250	0.07×10^{-3}	0.94	0.08×10^{-3}	0.94
H_2	150	104.33	0.90	95.81	0.91
	200	96.48	0.92	107.92	0.90
	250	76.19	0.94	85.57	0.93

Table S8: Comparative between gas-sensing application metrics found in the literature and metrics of this work [1]:

Algorithm	Application	Metrics	References
SVM	Drift compensation, Classification	Accuracy: 89.98 % – 96.62 %	[2,3]

ANN	Classification	Accuracy: 91.26%	2
XGBoost	Classification	Accuracy: 96.62 % Sensitivity: 95.60 %	2,4
KNN	Drift compensation	Accuracy: 80.74 % – 97.5 %	2,5,6
KNN-ANN	Drift suppressed classification	Accuracy: 96.51 %	7
PLS	Gas concentration prediction	RMSE: 7.34	8,9
ACNN	Drift compensation	Accuracy increased over 30% worst case	10
MLPNN	Gas concentration estimation	Error decreased 7 % – 19 % worst case	11
Deep CNN	Real-time classification	Accuracy: 98.1 %	12
CNN ensemble	Classification	Accuracy: 99.72 %	13
PCA and ANN	Discrimination and Quantification	Accuracy: 96.1 % * R-squared: 0.96 * RMSE: 0.07 ppb *	This work

*Best case

References

1 Md. S. I. Sagar, N. R. Allison, H. M. Jalajamony, R. E. Fernandez and P. K. Sekhar, *J Electrochem Soc*, 2022, **169**, 127512.

2 T. Matthews, M. Iqbal and H. Gonzalez-Velez, in *2018 IEEE/ACM 5th International Conference on Big Data Computing Applications and Technologies (BDCAT)*, IEEE, 2018, pp. 61–70.

3 T. Liu, D. Li, J. Chen, M. Wu and Y. Chen, in *2018 5th International Conference on Systems and Informatics (ICSAI)*, IEEE, 2018, pp. 417–423.

4 K. Chen, L. Liu, B. Nie, B. Lu, L. Fu, Z. He, W. Li, X. Pi and H. Liu, *Comput Biol Med*, 2021, **131**, 104294.

5 C. Deng, K. Lv, D. Shi, B. Yang, S. Yu, Z. He and J. Yan, *Sensors*, 2018, **18**, 1909.

6 Z. Jiang, P. Xu, Y. Du, F. Yuan and K. Song, *Sensors*, 2021, **21**, 3403.

7 M. Abbatangelo, E. Núñez-Carmona, V. Sberveglieri, E. Comini and G. Sberveglieri, *Chemosensors*, 2020, **8**, 6.

8 L. Wozniak, P. Kalinowski, G. Jasinski and P. Jasinski, *Microelectronics Reliability*, 2018, **84**, 163–169.

9 J. Burgués, M. D. Esclapez, S. Doñate and S. Marco, *iScience*, 2021, **24**, 103371.

10 L. Feng, H. Dai, X. Song, J. Liu and X. Mei, *Sens Actuators B Chem*, 2022, **351**, 130986.

11 J. Wang, S. Lian, B. Lei, B. Li and S. Lei, *Sens Actuators A Phys*, 2022, **335**, 113392.

12 M. Kang, I. Cho, J. Park, J. Jeong, K. Lee, B. Lee, D. Del Orbe Henriquez, K. Yoon and I. Park, *ACS Sens*, 2022, **7**, 430–440.

13 S. Chaudhri and N. Rajput, *IEEE Sens Lett*, 2022, **6**, 1–4.